Journal of Controlled Release 399 (2026) 115339

Contents lists available at ScienceDirect

Journal of Controlled Release

journal homepage: www.elsevier.com/locate/jconrel

A liposomal inverse vaccine protects mice from arthritis and experimental autoimmune encephalomyelitis☆

Naomi Benne [a,*], Daniel Sáenz Fernández [a], Deja Porenta [a,b], Laura Bolkaerts [c,d], Arie Jan Stoppelenburg [a], Antoinette van den Dikkenberg [b], Teja Shyam Kankipati [e], Enrico Mastrobattista [b], Jerome J.A. Hendriks [c,d], Femke Broere [a,f]

[a] Section of Immunology, Division of Infectious Diseases and Immunology, Department of Biomolecular Health Sciences, Faculty of Veterinary Medicine, Utrecht University, Utrecht, the Netherlands
[b] Utrecht Institute for Pharmaceutical Sciences, Department of Pharmaceutics, Faculty of Science, Utrecht University, Utrecht, the Netherlands
[c] Department of Immunology and Infection, Biomedical Research Institute, Hasselt University, Diepenbeek, Belgium
[d] University MS Center Hasselt, Pelt, Belgium
[e] Section of Virology, Division of Infectious Diseases and Immunology, Department of Biomolecular Health Sciences, Faculty of Veterinary Medicine, Utrecht University, Utrecht, the Netherlands
[f] Department of Clinical Sciences, Faculty of Veterinary Medicine, Utrecht University, Utrecht, the Netherlands

ARTICLE INFO

Keywords:
Inverse vaccination
Anionic liposomes
Autoimmunity
Antigen-specific tolerance

ABSTRACT

Chronic autoinflammatory diseases such as rheumatoid arthritis and multiple sclerosis lack curative therapies, and current immunosuppressive treatments often cause systemic off-target effects. To address this unmet need, we previously developed an "inverse vaccine" based on anionic phosphatidylglycerol liposomes carrying a disease-specific peptide antigen conjugated to dexamethasone. Here, we assess the therapeutic efficacy and immunomodulatory mechanisms of this platform in two murine models of autoimmunity. In the proteoglycan-induced arthritis model, a single administration of liposomal dexamethasone-human proteoglycan peptide (Dex-K4-hPG) markedly slowed arthritis progression compared to an equivalent dose of free Dex-K4-hPG. Long-term follow-up showed that two injections provided superior protection over a single dose, whereas a third injection yielded no additional benefit. Flow cytometry of paw draining lymph nodes revealed reduced RORγt^{+}CD4^{+} T cells in mice receiving multiple doses indicating a shift toward less pro-inflammatory T-cell responses. Histological staining of the knees of mice also revealed less damage to the joints of mice receiving 2 or 3 injections of liposomes. To evaluate the versatility of this platform, we generated a novel Dex-peptide conjugate by replacing hPG for myelin oligodendrocyte glycoprotein (MOG). The resulting Dex-K4-MOG conjugate was encapsulated in the liposomes at high encapsulation efficiency (~60%), demonstrating platform modularity. In an experimental autoimmune encephalomyelitis mouse model, two injections of Dex-K4-MOG liposomes (one before disease induction and one after) strongly suppressed disease development compared with controls. Together, these findings demonstrate that antigen-specific inverse vaccination using anionic liposomes offers a modular and broadly applicable strategy for inducing long-term protection in multiple autoimmune disease models. The platform elicits regulatory immune signatures and suppresses pathogenic Th17 responses, supporting its potential as a tolerogenic therapeutic approach.

1. Introduction

Autoimmune diseases comprise a heterogeneous group of chronic disorders that arise when the immune system mounts inflammatory responses against auto-antigens, leading to chronic tissue inflammation. Under physiological conditions, the immune system employs multiple mechanisms to maintain tolerance to auto-antigens. Autoreactive T cells are largely eliminated during thymic selection, and those that escape into the periphery are suppressed by regulatory cell populations [1]. Among these, thymus-derived CD4^{+}FOXP3^{+} regulatory T (Treg) cells

☆ This article is part of a Special issue entitled: 'DDS for chronic and autoimmune diseases' published in Journal of Controlled Release.

* Corresponding author.
E-mail address: n.benne@uu.nl (N. Benne).

https://doi.org/10.1016/j.jconrel.2026.115339
Received 19 June 2026; Received in revised form 3 September 2026; Accepted 7 September 2026
Available online 8 September 2026

suppress effector T cells (Teff) cells directly, but also modulate Ag-presenting cells (APCs), sequester IL-2, and secrete immunoregulatory cytokines such as IL-10 and TGF-β [2]. In addition, peripherally induced type 1 regulatory T (Tr1) cells suppress autoreactive immune responses by secreting high levels of IL-10 and TGF-β [3]. Autoimmune diseases can manifest in different organs, depending on the auto-antigen. Rheumatoid arthritis (RA) is characterized by infiltration of pro-inflammatory immune cells into the synovium, resulting in synovial hyperplasia and destruction of bone and articular cartilage, ultimately causing pain, disability, and reduced quality of life [4]. Multiple sclerosis (MS), another prevalent autoimmune disorder, similarly involves auto-antigen-driven immune dysregulation, in this case targeting myelin within the central nervous system [5].

Despite the substantial burden of RA and MS, no curative therapies exist. Current treatments, including disease-modifying antirheumatic drugs (DMARDs), disease-modifying therapies (DMTs) for MS, non-steroidal anti-inflammatory drugs (NSAIDs), and corticosteroids, are broadly immunosuppressive and not antigen (Ag)-specific, leading to significant off-target effects and increased susceptibility to infections [6,7]. These limitations have motivated the development of next-generation therapeutic strategies aimed at restoring Ag-specific immune tolerance while preserving global immune function. Inverse vaccines have emerged as novel therapies that aim to induce Ag-specific immune tolerance [8–10]. One strategy is to encapsulate Ags (in combination with immunomodulatory compounds) in a drug delivery vehicle to be delivered to immune cells [11–16]. Lipid-based nanoparticles, including liposomes, are commonly used for this purpose. For example, incorporating a nuclear factor-κB (NF-κB) inhibitor and diabetes-specific Ag into L-α-phosphatidylcholine:L-α-phosphatidylglycerol liposomes generates DCs that induce Treg-cell differentiation, and subsequently reduces type 1 diabetes in mice [17]. Similarly, liposomes composed of dioleoylphosphatidylserine (DOPS):dimyristoylphosphatidylcholine (DMPC):cholesterol (CHOL) and encapsulating different auto-antigens have shown effectiveness at reducing symptoms in several autoimmune disease mouse models [18]. We previously demonstrated that dexamethasone (Dex)-Ag conjugates can be efficiently encapsulated into distearoylphosphatidylcholine (DSPC):distearoylphosphatidylglycerol (DSPG):CHOL liposomes. Dex-Ag liposomes induced IDO, TLR2, and IL-10 expression in dendritic cells (DCs), promoting Ag-specific Tr1s *in vitro* and *in vivo*. In the proteoglycan-induced arthritis (PGIA) model, liposomes carrying the disease-relevant Dex-human proteoglycan conjugate (Dex-K4-hPG) prevented disease onset and halted progression of established arthritis [15]. We have observed that IV-injected DSPC:DSPG:CHOL liposomes are taken up by macrophages, mainly in the liver and spleen, which indicate that our platform acts as an inverse vaccine that depends on the systemic induction of Ag-specific Tregs following APC uptake [19].

Building upon previous work, we investigated the versatility, long-term durability, and underlying mechanism of our inverse vaccination platform across two mechanistically distinct autoimmune disease models. Specifically, we evaluated therapeutic efficacy of Dex-K4-Ag liposomes in the PGIA and in the experimental autoimmune encephalomyelitis (EAE) mouse models and found that liposomes could protect mice from disease induction in both models. In the PGIA model, we further examined the effect of the dosing regimen (single *versus* multiple administrations) on the magnitude and durability of disease protection. To define the mechanistic basis of tolerance induction by this platform, we characterized the phenotype of liposome-treated DCs *in vitro* and assessed downstream effects on pathogenic and regulatory T cells population *in vivo*. Collectively, these studies were designed to determine whether Ag-specific inverse vaccination using anionic liposomes is a promising strategy capable of inducing durable immunological tolerance across multiple autoimmune disease models, and to provide mechanistic insight into how this tolerance is achieved.

2. Materials and methods

2.1. Dexamethasone-peptide conjugation

Preloaded Fmoc-Lys(Boc)-Wang and Fmoc-Arg(Pbf)-Wang resins, Fmoc-protected amino acids, and trifluoroacetic acid (TFA) were obtained from Novabiochem GmbH (Hohenbrunn, Germany). Peptide-grade dimethylformamide (DMF), dichloromethane (DCM), piperidine, N,N′-diisopropylcarbodiimide (DIC), and HPLC-grade acetonitrile were purchased from Biosolve BV (Valkenswaard, Netherlands). Ethyl cyanohydroxyiminoacetate (Oxyma Pure) was obtained from Manchester Organics Ltd. (Cheshire, UK). Triisopropylsilane (TIPS), BioUltra-grade ammonium bicarbonate, succinic anhydride, 4-dimethylaminopyridine (DMAP), and pyridine were sourced from Sigma-Aldrich Chemie BV (Zwijndrecht, Netherlands). Dexamethasone (Dex) was purchased from Acros Organics BV (The Hague, Netherlands). Dex–peptide conjugates were synthesized as previously described [15]. Briefly, peptide epitopes were purchased from GenScript (NJ, USA) or synthesized by microwave-assisted Fmoc solid-phase peptide synthesis using an H12 Liberty Blue peptide synthesizer (CEM Corporation, USA). Dex-succinate was coupled at the peptide N-terminus following standard Fmoc coupling procedures. Deprotection and resin cleavage were performed using TFA/water/TIPS (95:2.5:2.5, *v*/v/v). Crude products were purified by preparative HPLC on a Reprosil-Pur C18 column (10 μm, 250 × 22 mm). Product identity was confirmed by mass spectrometry (Bruker microTOF-Q, positive mode).

2.2. Liposome preparation

Liposomes were prepared by thin-film hydration followed by high-pressure extrusion. DSPC (Lipoid GmbH, Ludwigshafen am Rhein, Germany), DSPG (Avanti Polar Lipids, Birmingham, AL, USA), and cholesterol (Sigma-Aldrich, St. Louis, MO, USA) were combined at a 4:1:2 M ratio to a total amount of 180 mg lipid, which was transferred to a dry, sterile 50-mL round-bottom flask. Lipids were dissolved in 8 mL chloroform and 8 mL methanol, and the solvent was removed under reduced pressure using a rotary evaporator for 1 h at 40 °C. Residual solvent was eliminated by applying a nitrogen stream for 1 h at room temperature. The resulting lipid film was hydrated with 4 mL of 10 mM phosphate buffer (pH 7.4) containing 2000 μg of Dex-peptide conjugate and homogenized by gentle rotation in a 40 °C water bath for 1 h. Liposomal suspensions were subsequently extruded (LIPEX Extruder, Northern Lipids Inc., Burnaby, BC, Canada) at 60 °C through stacked 400- and 200-nm polycarbonate membranes (Whatman Nucleopore™, GE Healthcare), passing four times through each membrane. Non-encapsulated material was removed by ultracentrifugation (Type 70.1 Ti rotor, Beckman Coulter) at 55,000 rpm for 35 min at 4 °C. Pelleted liposomes were washed three times with 10 mL phosphate buffer and stored at 4 °C. Formulations were used within 2 weeks for *in vitro* and *in vivo* experiments.

2.3. Liposome characterization

Z-average diameter and polydispersity index (PDI) was measured by dynamic light scattering (NanoZS Zetasizer, Malvern Instruments, Malvern, UK) after diluting 10 μL liposomes in 990 μL phosphate buffer (pH 7.4). ζ-Potential was measured by laser Doppler electrophoresis using a universal dip cell (Malvern Instruments). Encapsulated Dex-peptide conjugate was quantified by reversed-phase UPLC (Waters ACQUITY UPLC System). Liposomes (20 μL) were solubilized in 180 μL methanol, vortexed, and injected (7.5 μL) onto a BEH C18 column (1.7 μm, 2.1 × 50 mm). Column and sample temperatures were maintained at 40 °C and 20 °C, respectively. Separation was achieved using a linear gradient from 5 to 95% acetonitrile (0.1% TFA) over 8 min at 0.25 mL/min. Detection was performed at 280 nm for peptide and 240 nm for Dex. Quantification was based on calibration curves generated from Dex-

peptide complexes prepared in methanol.

2.4. BMDC cell culture

Bone marrow was isolated from 8-week-old wild-type (WT) Balb/cAnNCrl mice (male and female; Charles River Laboratories). Bone marrow was flushed from femurs and tibias, homogenized, and plated in 6-well plates at 4.5×10^5 cells/mL in 2 mL Iscove's Modified Dulbecco's Medium (IMDM, Gibco) supplemented with 10% fetal calf serum (FCS; Bodinco), 100 U/mL penicillin, 100 μg/mL streptomycin (Gibco), and 0.5 μM β-mercaptoethanol (Gibco). Cells were cultured at 37 °C and 5% CO_2 in the presence of 20 ng/mL granulocyte–macrophage colony-stimulating factor (GM-CSF, Biolegend) for 6 days. On day 2, fresh IMDM containing 20 ng/mL GM-CSF was added, and an additional 20 ng/mL GM-CSF was supplemented on day 5. On day 6, the resulting DCs were harvested by gentle scraping, counted, and transferred to 96-well F-bottom plates at 5×10^4 cells per well. After a 2 h adherence period, DCs were matured with 10 ng/mL lipopolysaccharide (LPS, O111:B4, Sigma-Aldrich) and treated with free K4-Ag, free Dex, or free or encapsulated Dex-K4-Ag (200 μL per well). Free Dex was added at a concentration equimolar to the Dex content of the Dex-K4-Ag conjugate. After 16 h, DCs were collected for phenotypic analysis by flow cytometry. For qPCR, cells were seeded at 6×10^5 cells per well in 48-well F-bottom plates and allowed to adhere for 2 h prior to stimulation (total volume 600 μL per well).

2.5. moDC cell culture

Peripheral blood mononuclear cells (PBMCs) were obtained from healthy donors through the Sanquin Blood Bank (Amsterdam, the Netherlands). Written informed consent was obtained in accordance with the Declaration of Helsinki and institutional ethics approval. PBMCs were isolated by Ficoll density gradient, and monocytes were purified using anti-CD14 microbeads (Miltenyi Biotec) following the manufacturer's protocol. Monocytes were seeded in 6-well plates at 2×10^6 cells/mL in 2 mL RPMI 1640 (Gibco) supplemented with 5% FCS (Bodinco), 100 U/mL penicillin, and 100 μg/mL streptomycin (Gibco). Differentiation into monocyte-derived dendritic cells (moDCs) was induced by adding 50 ng/mL human GM-CSF (Miltenyi Biotec) and 50 ng/mL human IL-4 (Miltenyi Biotec). On day 3, half of the medium was replaced with fresh cytokine-supplemented medium. On day 6, cells were harvested by scraping, counted, and plated in 96-well F-bottom plates at 5×10^4 cells per well. After 2 h adherence, cells were matured with 100 ng/mL LPS (O111:B4, Sigma-Aldrich) and treated with free or encapsulated K4-Ag, or free or encapsulated Dex-K4-Ag (200 μL per well). Peptide and Dex concentrations were 1 μg/mL peptide and 0.18 μg/mL Dex. After 16 h, cells were collected for flow-cytometric analysis. For ELISA, cells were seeded at 6×10^5 cells per well in 48-well F-bottom plates and allowed to adhere for 2 h prior to stimulation (total volume 600 μL per well).

2.6. In vivo liposome efficacy in PGIA mouse model

For PGIA experiments, retired breeder female Balb/cAnNCrl mice were obtained from Charles River Laboratories. Animals were randomly allocated to experimental groups on the basis of body weight RandoMice [20]. Humane endpoints were strictly applied. To reduce discomfort in arthritic mice, easily accessible food and water as well as additional soft bedding were provided. All mice were housed under standard conditions, and all procedures were approved by the Utrecht University Animal Experiment Committee (AVD108002016467 and AVD10800202115687). Arthritis was induced in mice by intraperitoneal injection on days 0 and 21 with a suspension containing 2 mg dimethyldioctadecylammonium bromide (DDA) and 250 μg human proteoglycan. Mice received treatment by intravenous injection *via* the tail vein. An untreated (disease-only) control group was not included in this study. However, disease induction and progression in this model have been extensively characterized in our previous work [8,15]. Arthritis severity was scored three times weekly from day 21 until the end of the experiment by two independent, blinded observers using a validated visual scoring system assessing paw swelling and erythema. Arthritis scoring ranged from 0 to 4 per paw in 1-point increments, to a total possible score of 16 per mouse (0: normal paw, 1: mild swelling and/or redness limited to a single digit or the wrist/ankle, 2: moderate swelling and redness extending to multiple digits or the entire paw, 3: severe swelling, redness, and inflammation affecting the entire paw, 4: maximum inflammation, severe swelling, and joint deformity and stiffness [21]. For ethical reasons, the control group (Dex-K4-hPG) was sacrificed on day 55, which prevented mice from reaching the humane end-point, which was set at a score of 12. At study termination, mice were euthanized by cervical dislocation, and spleens, popliteal lymph nodes (pLNs), and knee joints were collected.

2.7. In vivo liposome efficacy in experimental autoimmune encephalomyelitis (EAE) mouse model

For the EAE experiment, 11-week-old female C57BL/6 J mice were purchased from Envigo. Animals were housed on a 12 h light/dark cycle with *ad libitum* access to standard chow diet and water. The EAE experiment was conducted in accordance with the institutional guidelines and approved by the Ethical Committee for Animal Experiments of Hasselt University (protocol number 202434A1). To induce EAE, mice were injected subcutaneously with 200 μg myelin oligodendrocyte glycoprotein peptide ($MOG_{35–55}$) emulsified in 200 μL complete Freund's adjuvant with *Mycobacterium tuberculosis* (heat-inactivated) according to the manufacturer's guidelines (EK-21110 kit, Hooke laboratories). Immediately after immunization and 24 h later, mice were injected intraperitoneally (i.p.) with 110 ng pertussis toxin (EK-21110 kit, Hooke laboratories). Mice were injected intravenously 4 days before and 2 days after EAE induction with vehicle (saline), empty liposomes, dex-K4-MOG (2 nmol), or dex-K4-ovalbumin (Dex-K4-OVA) (2 nmol) encapsulated in liposomes. Mice were weighed and evaluated for neurological signs of the disease daily in a blinded fashion according to the manufacturer's mouse EAE scoring guide with scores ranging from 0 to 5 in 0.5-point increments (0: no clinical symptoms; 1: tail paralysis; 2: tail paralysis and partial hind limb paralysis; 3: complete hind limb paralysis; 4: paralysis to the diaphragm; 5: death by EAE). At the end of the experiment, mice were sacrificed with a lethal dose of dolethal (200 mg/kg, i.p.)

2.8. Organ processing

Single-cell suspensions of spleen and pLNs were prepared by gently dissociating the tissue through a 70 μm cell strainer (Falcon, Corning, New York, USA). Red blood cells from spleens were lysed using ammonium–chloride–potassium (ACK) lysis buffer (0.15 M NH_4Cl, 1 mM $KHCO_3$, 0.1 mM Na_2EDTA; pH 7.3). After lysis, cells were washed and counted for downstream applications. To isolate knees, the femur and tibia were cleaned and cut just above and below the knees.

2.9. Flow cytometry

BMDCs or moDCs were stimulated as described above, harvested, and washed three times with 200 μL 4 mM EDTA followed by one wash with 200 μL PBS to remove residual Ag or liposomes. Cells were then transferred to V-bottom 96-well plates. For splenocytes obtained from *in vivo* experiments, 2×10^6 cells were plated into U-bottom 96-well plates. pLNs were divided over two wells. Mouse cell suspensions were incubated with Fc Block (10 μg/mL; clone 2.4G2, produced in-house) for 15 min to prevent nonspecific antibody binding. Surface staining was performed in FACS buffer (PBS containing 2% FCS, 0.01% sodium azide, and 2 mM EDTA) at a total volume of 50 uL/well. BMDCs were stained

with the following monoclonal antibodies: CD11c-APC (N418, eBioscience), CD86-FITC (GL1, BD Biosciences), MerTK-APC (2B10C42, BioLegend), and ViaKrome808 (Beckman Coulter). moDCs were stained with: CD11c-PE (MJ4-27G12, Miltenyi), CD83-Pe-Vio770 (HB15, Miltenyi), TLR2-FITC (TL2.1, eBioscience), and ViaKrome808 (Beckman Coulter). Splenocytes and pLNs were stained with CD25-PerCP-Cy5.5 (PC61.5, eBioscience), CD8-V500 (I.83, BD Biosciences), PD-1-FITC (J43, eBioscience), LAG-3-PE (eBioC9B7W, eBioscience), CD4-BV785 (RM4–5, Biolegend), and ViaKrome 808 (Beckman Coulter). After 30 min incubation at 4 °C in the dark, cells were washed with PBS, and fixed and permeabilized using the FoxP3 Transcription Factor Staining Buffer Set (eBioscience). Intracellular staining was performed according to the manufacturer's instructions using Foxp3-eF450 (FJK-16 s, eBioscience) and RORγT-PE-Cy7 (Q31–378, BD Biosciences). Following intracellular staining (30 min at 4 °C in the dark), cells were washed and resuspended in 100 μL PBS for acquisition. Single-stain and fluorescence-minus-one (FMO) controls were included for all analyses. Samples were recorded on a Beckman Coulter CytoFLEX LX flow cytometer (Flow Cytometry and Cell Sorting Facility, Faculty of Veterinary Medicine, Utrecht University). A total volume of 85 μL per sample was acquired at 60 μL/min. Data was analyzed using FlowJo v10.7 (FlowJo LLC).

2.10. ELISA

moDCs were stimulated as described above, and culture supernatants were collected and either analyzed immediately or stored at −80 °C until use. The concentrations of TNF-α were quantified by ELISA following the manufacturers' protocols (ThermoFisher Scientific). Briefly, F-bottom 96-well Costar assay plates (Corning) were coated overnight at 4 °C with the appropriate capture antibody. After washing with PBS containing 0.01% Tween-20, plates were blocked with 1% BSA in PBS for 30 min at room temperature (RT). Diluted samples and standard curves were then added and incubated for 2 h at RT. Following additional washing steps, biotinylated detection antibodies were applied for 1 h at RT. This was washed again, and streptavidin–HRP (BD Biosciences) was added for 1 h at RT. Plates were washed again, developed with TMB substrate (BioLegend), and the reaction was stopped with 2 N H_2SO_4. Absorbance was measured using an iMark Microplate Absorbance Reader (Bio-Rad). Cytokine concentrations were calculated from standard curves generated with recombinant cytokines.

2.11. qPCR

BMDCs were stimulated as described above, after which 350 μL RLT buffer (Qiagen) was added to each well. Lysates were processed immediately or stored at −80 °C. Total RNA was extracted using the RNeasy Kit (Qiagen) with on-column DNase digestion. RNA yield and purity were assessed using a Nanodrop spectrophotometer (ThermoFisher). cDNA was synthesized from purified RNA using the iScript cDNA Synthesis Kit (Bio-Rad). Quantitative PCR was performed on a Bio-Rad MyiQ iCycler using iQ SYBR Green Supermix (Bio-Rad) with final primer concentrations of 0.25 μM. Gene expression was assessed for *IL10* (5′-GGT TGC CAA GCC TTA TCG GA-3′; 5’-ACC TGC TCC ACT GCC TTG CT-3′), *IL12B* (5′-GGA AGC ACG GCA GCA GAA TA-3′; 5’-AAC TTG AGG GAG AAG TAG GAA TGG-3′), *NFKB* (5’-GCT GCC AAA GAA GGA CAC GAC A-3′; 5’-GGC AGG CTA TTG CTC ATC ACA G-3′) and the housekeeping gene *HPRT* (5′-CTG GTG AAA AGG ACC TCT CG-3′; 5′-TGA AGT ACT CAT TAT AGT CAA GGG CA-3′). The PCR program consisted of an initial denaturation at 95 °C for 3 min, followed by 40 cycles of 95 °C for 20 s and 59 °C for 30s. Melting curves and primer efficiencies were assessed for each run. Relative gene expression was normalized to HPRT Ct values and calculated using the ΔΔCt method, expressed relative to BMDCs stimulated with K4-Ag + LPS.

2.12. Histopathology

Knees were fixed in 4% formalin at 4 °C overnight. Then, knees were decalcified in 10% EDTA at 4 °C for 3 weeks. Samples were embedded in paraffin and sagittal sections were cut and stained with hematoxylin and eosin. The stained samples were evaluated and scored for inflammation by two blinded evaluators. Scoring was as follows: 0 = normal, 1 = minimal infiltration of inflammatory cells in the synovial and/or periarticular tissues, 2 = mild infiltration with mild edema, 3 = moderate infiltration (including joint space) with moderate edema, 4 = marked infiltration with marked edema, and 5 = severe infiltration with severe edema [22,23].

2.13. Statistical analysis

Statistical analysis was performed in GraphPad Prism v.10.4.1. Details of the analyses are indicated in the figure legends.

3. Results

To test the versatility of the liposome platform, we prepared liposomes encapsulating a range of peptide antigens (Table 1). We selected known auto-antigens and chemically linked them to dexamethasone using a polylysine linker. All Dex-K4-Ag were efficiently encapsulated (45.6–61.6%). The resulting liposomes had similar sizes (191.8–199.7 nm), low PDI (0.061–0.075) and were negatively charged (−46.0–60.7 mV). Liposomes were stable over a period of at least 18 months (Fig. S1). EM data showed a characteristic collapsed, cup-shaped morphology typical of negative-stain sample preparation (Fig. S2).

Next, we tested whether liposomal Dex-K4-Ag could induce a tolerogenic phenotype in DCs. Dex-K4-Ag liposomes reduced the frequency of $CD86^+CD11c^+$ BMDCs (Fig. 1A and Fig. S3A) while increasing $MerTK^+CD11c^+$ cells (Fig. 1B and Fig. S3B) in a concentration-dependent manner. While free Dex-K4-Ag decreased *IL12B* compared to free Ag, encapsulation in liposomes significantly increased *IL10* expression and reduced *NFKB* expression compared with both free Ag or free Dex-K4-Ag (Fig. 1C-E). We further assessed these liposomes in human monocyte-derived DCs (moDCs) and observed a similar tolerogenic effect; free and liposomal Dex-K4-Ag reduced CD83 (Fig. 2A) and increased TLR2 expression, with liposomal encapsulation further enhancing TLR2 expression (Fig. 2B). moDCs stimulated with liposomal Dex-K4-Ag also reduced LPS-induced TNF-α production (Fig. 2C).

We previously showed that Dex-K4-hPG encapsulated in liposomes could protect mice from PGIA compared to mice injected with PBS [15]. Here, we tested the effect of immunizing mice with the same amount of free or encapsulated Dex-K4-hPG. We induced PGIA in mice by IP injection of hPG and DDA on days 0 and 21, and immunized mice IV with 2 nmol free or liposomal Dex-K4-hPG on days 17 and 31. Only mice receiving the encapsulated Dex-K4-hPG had suppression of arthritis symptoms (Fig. 3A). Mice treated with free Dex-K4-hPG developed arthritis at a rate and severity comparable to previously reported untreated PGIA mice [8,15,24], confirming successful induction of disease in this model. To evaluate whether DSPC:DSPG:CHOL liposomes could induce tolerance in a different disease model, we used the EAE mouse model, an animal model of the neurodegenerative disorder MS. For this, mice were s.c. injected with $MOG_{35–55}$ and complete Freund's adjuvant followed by pertussis toxin injections. This induces infiltration of autoreactive T cells and macrophages into the central nervous system, resulting in progressive motor dysfunction [25]. Similar to the PGIA model, we observed a strong suppression of clinical symptoms in mice receiving liposomal Dex-K4-MOG compared to PBS only (Fig. 3B). In contrast, liposomes encapsulating an irrelevant Ag (Dex-K4-OVA) or empty liposomes did not confer protection, indicating Ag-specific therapeutic efficacy.

Next, we aimed to explore the effect of a single administration of Dex-K4-hPG liposomes *vs.* two or three injections. PGIA mice were

Table 1
Physicochemical characterization of DSPC:DSPG:CHOL liposomes carrying different dexamethasone-coupled (auto)antigens. $N = 3$.

Peptide sequence	(Auto)Ag	Size ± SD (nm)	PDI[a] ± SD	Z-potential ± SD (mV)	EE[b] ± SD (%)
Dex-KKKKISQAVHAAHAEINEAGR	Ovalbumin	192.3 ± 9.9	0.065 ± 0.024	−49.8 ± 5.6	45.6 ± 4.0
Dex-KKKKVLRIINEPTAAAIAY	HSP70[c]	199.7 ± 5.3	0.072 ± 0.017	−46.0 ± 4.2	58.0 ± 1.6
Dex-KKKKATEGRVRVNSAYQDK	hPG[d]	192.0 ± 8.5	0.065 ± 0.039	−56.3 ± 4.5	42.3 ± 7.1
Dex-KKKKMEVGWYRSPFSRVVHLYRNGK	MOG[e]	191.8 ± 11.6	0.061 ± 0.020	−51.7 ± 5.0	55.9 ± 3.3
Dex-KKKKGAGSLQPLALEGSLQKRG	Insulin	193.7 ± 14.8	0.075 ± 0.025	−56.4 ± 0.7	61.6 ± 1.2
Dex-KKKKVIVELIPSTSSAV	AChR[f]	193.3 ± 7.5	0.067 ± 0.041	−60.7 ± 1.4	51.4 ± 6.0

[a] PDI = polydispersity index.
[b] EE = encapsulation efficiency, % antigen in final formulation compared to amount added.
[c] Heat-shock protein 70.
[d] Human proteoglycan.
[e] Myelin oligodendrocyte glycoprotein.
[f] Acetylcholine receptor.

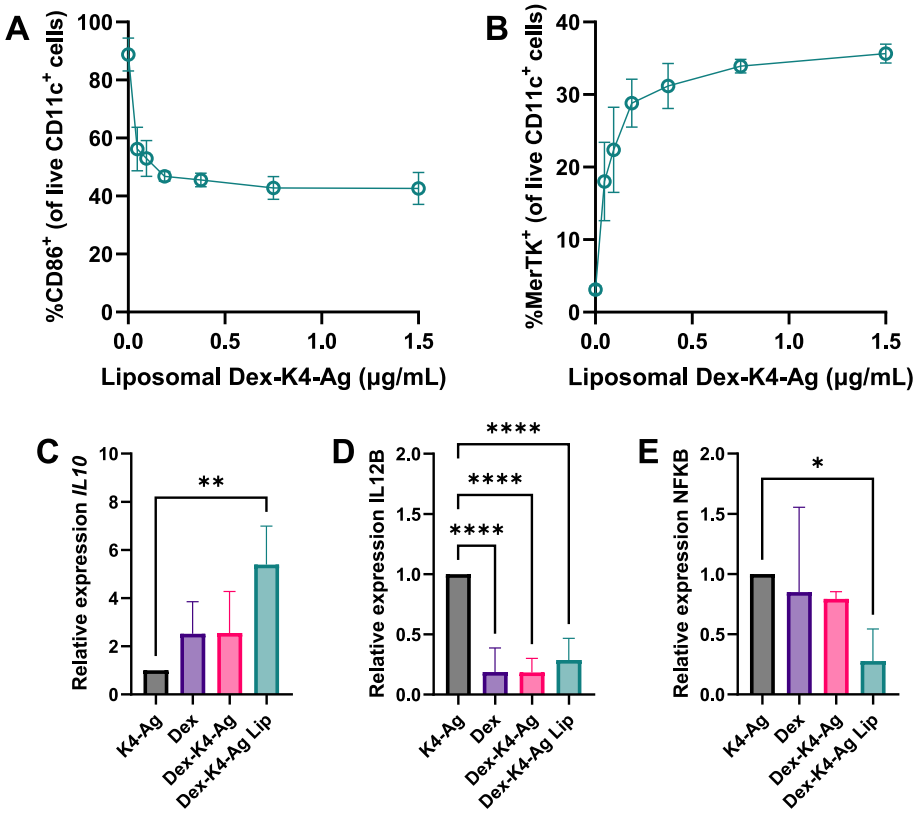

Fig. 1. Dex-K4-antigen, free or encapsulated in DSPC:DSPG:CHOL liposomes, induces a tolerogenic phenotype in Balb/cAnNCrl BMDCs. Immature BMDCs cultured from the bone marrow of Balb/cAnNCrl mice were stimulated overnight with LPS and different concentrations of Dex-K4-Ag liposomes. (A) %CD86$^+$CD11c$^+$ cells, (B) %MerTK$^+$CD11c$^+$ cells as determined by flow cytometry. BMDCs were incubated overnight with LPS in the presence of either K4-Ag, Dex, Dex-K4-Ag, or Dex-K4-Ag encapsulated in liposomes (Lip) at a concentration of 1 µg/mL antigen. The relative expression of *IL10*, *IL12B*, and *NFKB* were measured by qPCR. Means (+ SD), $n = 3$, * $p < 0.05$, ** $p < 0.01$, *** $p < 0.001$, **** $p < 0.0001$ as determined by one-way ANOVA and Bonferroni's multiple comparisons test.

injected with hPG and DDA on days 0 and 21, and received liposomes or PBS on days 17, 31, and 61. While a single injection of liposomes protected mice from developing arthritis (55% of mice had arthritis symptoms compared to 100% of controls, Table S1), and delayed the onset of disease (Table S1), multiple injections conferred greater protection (Fig. 4A-B). In the draining pLNs, multiple injections also reduced the number of RORγT$^+$CD4$^+$ Th17 cells, compared to a single injection (Fig. 4C). We found no additional benefit of the third injection over the second injection and observed no differences in splenic T cell effects, or suppressive CD4$^+$ T cell subsets (LAG3$^+$, PD-1$^+$, or CD25$^+$Foxp3$^+$, Fig. S4) when comparing the different liposome-treated groups. Compared to mice treated with free Dex-K4-hPG, however, mice receiving liposomal Dex-K4-hPG showed increased frequencies of splenic CD25$^+$Foxp3$^+$, LAG3$^+$, and PD-1$^+$ CD4$^+$ T cells, consistent with expansion of regulatory T cell subsets in liposome-treated mice. Histological analysis showed that multiple liposomal injections protected mice from damage to knee cartilage (Fig. 4D, Fig. S5).

4. Discussion & conclusion

Autoimmune diseases affect a large part of the population, and their prevalence has increased in the last years [26,27]. Currently, the lack of Ag-specific treatments necessitates patients to rely on broadly immunosuppressive treatments that have off-target effects [7,28,29]. Although Ag-specific approaches have been in development for the past years (*e.g.* oral or intradermal administration of auto-antigens or cell transfers), all of them have lacked efficacy, mainly due to fast elimination of the antigens or Ag-specific cells used in the therapy [1]. In this

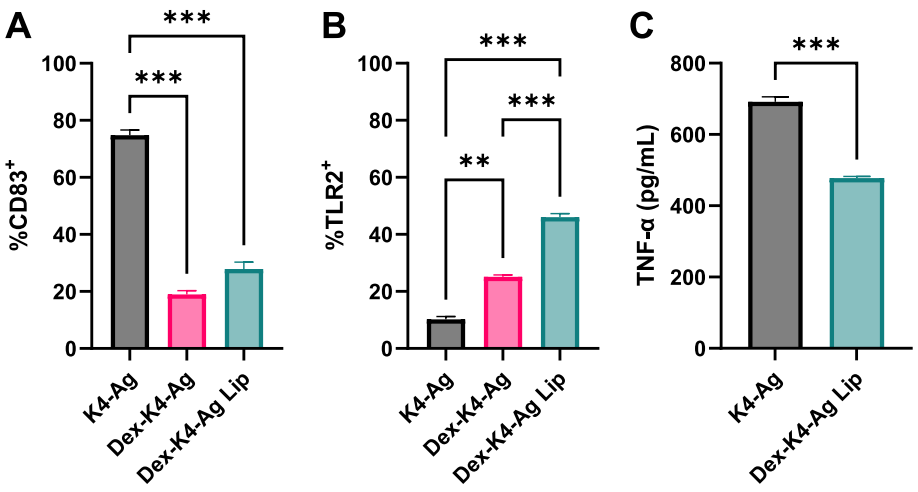

Fig. 2. Dex-K4-Ag, free or encapsulated in DSPC:DSPG:CHOL liposomes, induces a tolerogenic phenotype in moDCs. Human moDCs cultured from $CD14^+$ cells isolated from buffy coats of healthy donors were stimulated overnight with LPS and either K4-Ag, Dex-K4-Ag, or Dex-K4-Ag encapsulated in liposomes at a concentration of 1 μg/mL antigen. (A) $\%CD83^+$ $CD11c^+$ cells, (B) $\%TLR2^+$ $CD11c^+$ cells as measured by flow cytometry. (C) Release of TNF-α as measured by ELISA. Means (+ SD), $n = 3$, * $p < 0.05$, ** $p < 0.01$, *** $p < 0.001$, **** $p < 0.0001$ as determined by one-way ANOVA and Bonferroni's multiple comparisons test.

study, we examined the efficacy and durability of a liposome-based Ag-specific treatment aiming to induce tolerance *in vivo* in the context of autoimmune diseases. First, we formulated liposomes encapsulating a range of auto-antigens and evaluated their tolerogenic capacity in BMDCs and moDCs. Secondly, we analyzed the efficacy of the liposomes in *in vivo* models of PGIA and EAE. Finally, we addressed the duration of the tolerogenic activity of the liposomal treatment in an *in vivo* PGIA model by comparing different dosing regimes.

As shown in Table 1, the EE of the different Dex-K4-Ag complexes was between 42.3% and 61.6%. All liposomes had low PDI and were below 200 nm in size, which is desirable for efficient drug delivery and uptake by APCs [19,30–32]. The liposomes had negative ζ-potential (−46.0 mV to −60.7 mV) consistent with the anionic DSPG-containing lipid composition previously established by our group for induction of antigen-specific regulatory T cell responses. Other groups have also reported that an anionic nanoparticle encourages tolerance induction [14,33–39]. We aknowledge that a direct causal link between this specific ζ-potential range and cellular uptake was not evaluated in the present study. We can conclude that the choice of antigen has minimal effects on liposomal physicochemical properties, and that the liposomal platform is therefore widely applicable to a range of antigens.

BMDCs treated with our formulations show a dose-dependent tolerogenic trend indicated by a reduced expression of activation marker CD86 and an increase of tolerance marker MerTK (Fig. 1A-B). This effect on MerTK is likely due to the presence of dexamethasone and increases the DC's capacity to induce T cell tolerance [40–45]. At 1 μg/mL Ag, we observe an upregulation of *IL10* and downregulation of *IL12B* and *NFKB* in BMDCs stimulated with Dex-K4-Ag liposomes compared to free K4-Ag (Fig. 1C-E). The expression of *NFKB* mRNA was also reduced compared to BMDCs stimulated with free Dex-K4-Ag, which indicates an added benefit of the liposomal formulation to the Dex-K4-Ag. In moDCs, Dex-K4-Ag liposome stimulated cells had a reduced percentage of CD83 expressing cells and an increased percentage of TLR2 expressing cells compared to controls (Fig. 2A-B). We observe again that the liposomal formulation offers an added effect to the free Dex-K4-Ag conjugate, showing a higher frequency of TLR2 expressing moDCs. It was previously shown that glucocorticoids increase TLR2-expression in DCs [46]. Liposome-stimulated cells also reduced TNF-α secretion compared to free K4-Ag (Fig. 2C). These results align with previous studies that show that dexamethasone stimulated DCs have a tolerogenic phenotype [41,47].

We subsequently performed *in vivo* experiments to study the effects of our nanoparticles in the context of RA and MS. The PGIA mouse model is characterized by the development of polyarthritis and ankylosing spondylitis. This model depends on both antibodies and T cells, resembling human RA better than other used models such as collagen-induced arthritis [24]. EAE is the most commonly used MS mouse model and is mainly characterized by demyelination of the central nervous system mediated by CD4+ T cells [48]. Both models are induced in different mouse strains (BALB/c mice for PGIA and C57BL/6 for EAE). In the PGIA model, mice treated with two IV injections of Dex-K4-hPG liposomes were protected against the development of RA symptoms compared to mice treated with the same dose of free Dex-K4-hPG (Fig. 3A).This suggests that liposomal encapsulation enhances the tolerogenic potency of the Dex-K4-hPG conjugate, consistent with our *in vitro* DC phenotyping data showing a stronger tolerogenic effect of the encapsulated conjugate relative to the free conjugate. We propose that this reflects preferential uptake of the liposomal formulation by APCs in the spleen and liver, as recently characterized for DSPC:DSPG:CHOL liposomes of the same composition following intravenous administration [19], rather than prolonged systemic persistence of the formulation. In the EAE mouse model, we observe a significant reduction of the disease score only in mice treated with two IV injections of Dex-K4-MOG liposomes. In contrast, neither empty liposomes or Dex-K4-OVA liposomes had any effect on the symptoms, demonstrating an Ag-specific tolerogenic effect of the formulation (Fig. 3B). As an inverse vaccine, the therapeutic mechanism of this platform is expected to depend on systemic induction of antigen-specific Tregs following APC uptake, rather than on direct accumulation of the liposomal formulation at the site of inflammation (*e.g.*, the inflamed joint or CNS). However, local biodistribution to inflamed tissue was not evaluated in this study and can therefore not be excluded. Previous studies also show efficacy of inverse vaccination in EAE mice with different delivery formats, highlighting the strength of this technique [49,50]. Taking both experiments together, we demonstrated that our platform is efficient in tackling symptoms of autoimmune diseases in an Ag-specific manner, and, at the same time, is flexible enough to be modified to adapt the formulation to different diseases.

Our findings add to a growing body of work exploring particle-based inverse vaccines for antigen-specific tolerance in autoimmune diseases. For example, phosphatidylserine-rich liposomes targeting macrophages have been explored for type 1 diabetes [13], while liver-targeting mRNA-lipid nanoparticles have been used to induce tolerance in food allergy [51], and mesoporous silica-based vaccines have re-established tolerance in EAE [52]. Anionic lipid nanoparticles have also been shown to redirect biodistribution toward the spleen and preferentially

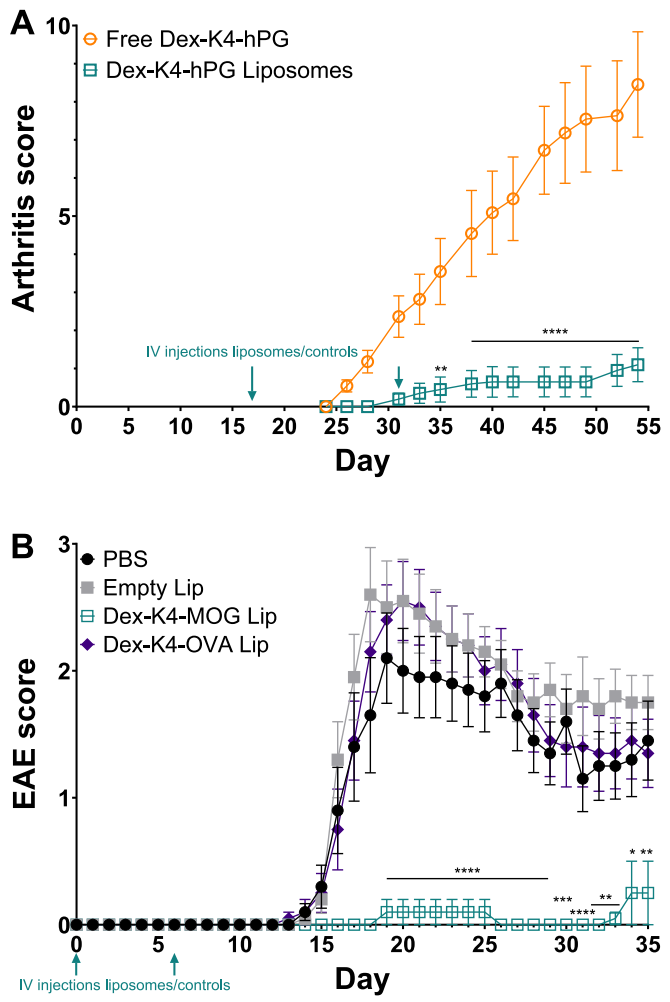

Fig. 3. Two injections of Dex-autoantigen conjugate-carrying DSPC:DSPG:CHOL protect mice against the development of autoimmunity. Disease severity was determined by a visual scoring system. (A) Female Balb/cAnNCrl mice ($n = 11$) were injected i.p. on days 0 and 21 with a mixture of 2 mg DDA and 250 μg human proteoglycan to induce arthritis. Mice were treated on days 17 and 31 *via* intravenous injection of 2 nmol free Dex-K4-hPG, or 2 nmol Dex-K4-hPG encapsulated in liposomes. Means ± SEM, ** $p < 0.01$, **** $p < 0.0001$ compared to free Dex-K4-hPG. (B) Female C57BL/6 J mice ($n = 10$) were injected s.c. with MOG peptide in CFA and injected i.p. with pertussis to induce EAE. Mice were treated on days 0 and 6 with PBS, 2 nmol Dex-K4-MOG encapsulated in liposomes, 2 nmol Dex-K4-OVA encapsulated in liposomes, or the equivalent lipid concentration of free liposomes (denoted by arrows). Means ± SEM, * $p < 0.05$, ** $p < 0.01$, *** $p < 0.001$, **** $p < 0.0001$ compared to PBS group as determined by two-way ANOVA and Bonferroni's multiple comparisons test.

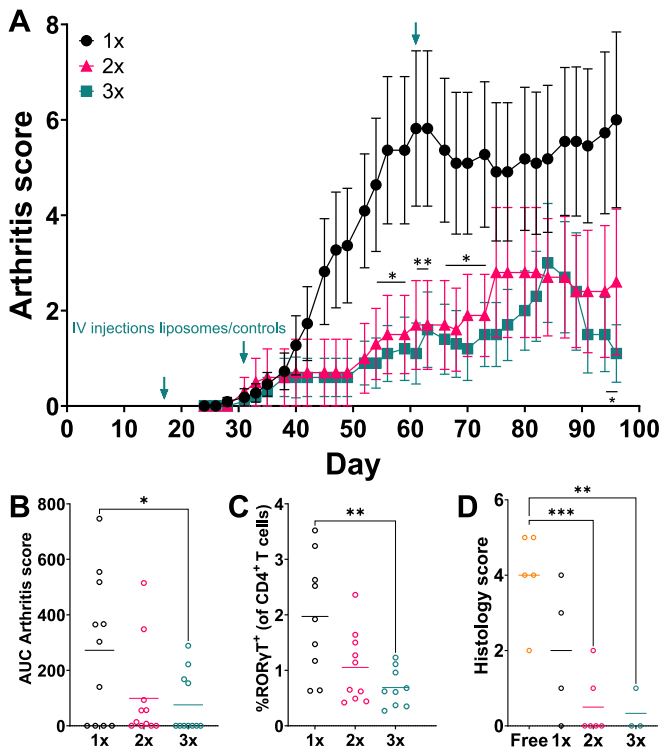

Fig. 4. The long-term effect of 1, 2, or 3 injections of Dex-K4-hPG liposomes on arthritis development. Female Balb/cAnNCrl mice were injected i.p. on days 0 and 21 with a mixture of 2 mg DDA and 250 μg human proteoglycan to induce arthritis. Mice were treated on day 17 with 2 nmol Dex-K4-hPG encapsulated in liposomes and on days 31 and 61 with PBS (1×), on days 17 and 31 with 2 nmol Dex-K4-hPG liposomes and on day 61 with PBS (2×), or on days 17, 31, and 61 with 2 nmol Dex-K4-hPG liposomes (3×, denoted by arrows). (A) Disease severity was determined by visual scoring. Means ± SEM, * $p < 0.05$, ** $p < 0.01$ comparing 3 injections to 1 injection as determined by two-way ANOVA and Bonferroni's multiple comparisons test. (B) Area under the curve of arthritis score for the duration of the study. Means ± SD, * $p < 0.05$ as determined by one-way ANOVA and Bonferroni's multiple comparisons test. (C) %RORγT$^+$ CD4$^+$ T cells in the popliteal lymph nodes on day 96. (D) Histology score of H&*E*-stained knees of mice on day 55 (PBS), or day 96 (1×, 2×, 3×). Means ± SD, * $p < 0.05$, ** $p < 0.01$, *** $p < 0.001$ as determined by one-way ANOVA and Bonferroni's multiple comparisons test.

transfect antigen-presenting dendritic cell subsets [39], consistent with the APC-targeting mechanism proposed for our own platform. Notably, antigen-specific nanoparticle platforms have already progressed to early-phase clinical trials: a liposomal peptide/calcitriol formulation showed tolerizing activity in a Phase I trial in ACPA-positive rheumatoid arthritis [12], and PLGA nanoparticles encapsulating gliadin (TAK-101) reduced gluten-specific immune activation in a Phase 1/2a trial in celiac disease, supporting the translational feasibility of antigen-specific, particle-based tolerance induction [53]. While liposomal platforms such as the one described here offer advantages in formulation flexibility, polymeric inverse vaccines have advanced further toward clinical translation, and PLGA particles are FDA-approved [54]. Continued development of liposomal inverse vaccines, including the platform described here, will benefit from parallel advances in scalable manufacturing and long-term stability characterization to support similar clinical translation.

In order to evaluate the duration of the effects of the treatment, we compared different numbers of IV doses of Dex-K4-hPG liposomes in PGIA mice. We observe a waning of the effects in mice receiving one dose of the treatment around 7 days after the last injection, compared to the mice treated with two or three doses which remained disease-free until the end of the experiment (Fig. 4A-B). It should be noted that even a single injection greatly limits the disease severity compared to no treatment. Interestingly, we observed no differences at any time points between mice receiving 2 or 3 injections of liposomes. Thus, two doses offer sufficient protection against the disease at least until day 96 in PGIA mice. The lack of additional benefit from a third injection may be similar as conventional prime-boost vaccination strategies, in which an initial boost is critical for establishing a robust response while further boosting within a short interval provides diminishing returns; a later, more widely spaced third injection might yield additional benefit and could be interesting for future study. Other studies have followed disease symptoms for between 30 and 55 days [9,55–59], so the timeframe presented here is long. At the end of the experiment, in the pLNs, there is a significant reduction of RORγT+ CD4+ T cells in the mice injected with more than one dose compared to those injected with one dose

(Fig. 4C). RORγT is the master transcription factor of Th17 cells, one of the main drivers of RA. Th17-derived cytokines, like IL-17, IL-21, or IL-23 appear to activate synovial fibroblasts and macrophages and their plasma levels are associated with higher disease activity [60–62]. Thus, a reduction in their frequency in the pLNs might be associated with the lower arthritis score of these two groups of mice. The fact that we can measure this response at such a late time-point in the study suggests durable effects possibly *via* long-term memory responses. This is consistent with the rapid systemic clearance of liposomes of the same composition following intravenous administration, as shown by our group using single-cell biodistribution analysis (undetectable in circulation by 24 h post-injection) [19], supporting a mechanism in which durability of protection reflects immunological memory rather than persistence of the liposomal formulation itself. At the histological level, we observe a significant prevention of knee joint damage with two and three injections compared to one injection, confirming efficacy of the treatment at the tissue level and the need for a booster injection to maintain tolerance (Fig. 4D).

Although this study introduces a promising platform to address RA and EAE, we did not further investigate how our liposomes compare with or could be used in addition to established treatment regimens for these diseases; exploring such combinations would be a valuable direction for future research. We also note that dose-response studies in the EAE model would be interesting for future work. In addition, treatment in the both models was administered prior to clinical symptom onset; while treatment timing in the PGIA model reflects a pre-symptomatic, seropositive disease stage relevant to clinical RA [24,63–65], the EAE treatment schedule does not fully replicate intervention at established disease and these results should be interpreted as evidence of preventive, rather than therapeutic, efficacy. Furthermore, in the long-term study on the PGIA model, we could not perform statistical analysis on the flow cytometry results compared to the untreated (PBS) group, as they were sacrificed at an earlier time-point than the liposome-treated mice. Although our models do not reflect the complexity of the disease in humans, they are widely used for drug development and thus provide a crucial first step into translating these results for human application. Further experiments with human (patient)-derived material are also essential to advance this therapy toward the clinic.

Our study demonstrates that induction of tolerance by dexamethasone coupled antigens provides a promising approach to treat autoimmune diseases.

Declaration of generative AI and AI-assisted technologies in the manuscript preparation process

The authors did not use AI in any part of this work.

CRediT authorship contribution statement

Naomi Benne: Writing – original draft, Visualization, Validation, Supervision, Methodology, Investigation, Funding acquisition, Formal analysis, Data curation, Conceptualization. **Daniel Sáenz Fernández:** Writing – original draft, Investigation. **Deja Porenta:** Writing – review & editing, Investigation. **Laura Bolkaerts:** Writing – review & editing, Investigation. **Arie Jan Stoppelenburg:** Investigation, Funding acquisition. **Antoinette van den Dikkenberg:** Validation, Methodology. **Teja Shyam Kankipati:** Visualization, Methodology, Investigation. **Enrico Mastrobattista:** Writing – review & editing, Supervision, Resources, Funding acquisition. **Jerome J.A. Hendriks:** Writing – review & editing, Conceptualization. **Femke Broere:** Writing – review & editing, Supervision, Resources, Funding acquisition, Conceptualization.

Funding sources

This work was funded by The Dutch Arthritis Foundation, FWO Vlaanderen (1SH6G24N), and Utrecht Holdings.

Declaration of competing interest

Authors N.B. and F.B. are inventors of patent application WO2025083024A1, held by Utrecht University. The IP license to this patent family is now held by Tolvac Therapeutics, a company founded by A.J.S. that was not a party to this study. A.J.S. has a financial interest in Tolvac Therapeutics. N.B. and F.B. have consulting roles with Tolvac. The other authors declare that they have no conflict of interest.

Acknowledgements

We would like to thank Dr. I. S. Ludwig and Dr. L. Timmermans for assistance with *in vivo* experiments. We would like to thank Dr. D. L. Hurdiss for advice and supervision relating to the negative-stain EM experiments.

Appendix A. Supplementary data

Supplementary data to this article can be found online at https://doi.org/10.1016/j.jconrel.2026.115339.

Data availability

Data will be made available on request.

References

[1] A. Page, F. Fusil, F.L. Cosset, Antigen-specific tolerance approach for rheumatoid arthritis: past, present and future, J. Bone Spine 88 (2021).
[2] C.Q. Xia, R. Peng, F. Beato, M.J. Clare-Salzler, Dexamethasone induces IL-10-producing monocyte-derived dendritic cells with durable immaturity, Scand. J. Immunol. 62 (2005) 45–54.
[3] J. Visser, A. Van Boxel-Dezaire, D. Methorst, T. Brunt, E.R. De Kloet, L. Nagelkerken, Differential regulation of interleukin-10 (IL-10) and IL-12 by glucocorticoids in vitro, Blood 91 (1998) 4255–4264.
[4] T. Rhen, J.A. Cidlowski, Antiinflammatory action of glucocorticoids — new mechanisms for old drugs, N. Engl. J. Med. 353 (2005) 1711–1723.
[5] N. Conrad, S. Misra, J.Y. Verbakel, G. Verbeke, G. Molenberghs, P.N. Taylor, J. Mason, N. Sattar, J.J.V. McMurray, I.B. McInnes, K. Khunti, G. Cambridge, Incidence, prevalence, and co-occurrence of autoimmune disorders over time and by age, sex, and socioeconomic status: a population-based cohort study of 22 million individuals in the UK, Lancet 401 (2023) 1878–1890.
[6] J.Y. Han, M.A. Reynolds, Effect of anti-rheumatic agents on periodontal parameters and biomarkers of inflammation: a systematic review and meta-analysis, J. Periodontal. Implant Sci. 42 (2012) 3–12.
[7] S. Shams, J.M. Martinez, J.R.D. Dawson, J. Flores, M. Gabriel, G. Garcia, A. Guevara, K. Murray, N. Pacifici, M.V. Vargas, T. Voelker, J.W. Hell, J.F. Ashouri, The therapeutic landscape of rheumatoid arthritis: current state and future directions, Front. Pharmacol. 12 (2021).
[8] D.T. Braake, N. Benne, C.Y.J. Lau, E. Mastrobattista, F. Broere, Retinoic acid-containing liposomes for the induction of antigen-specific regulatory T cells as a treatment for autoimmune diseases, Pharmaceutics 13 (2021).
[9] M.A.A. Jansen, R. Spiering, I.S. Ludwig, W. van Eden, C.M.U. Hilkens, F. Broere, Matured tolerogenic dendritic cells effectively inhibit autoantigen specific CD4+ T cells in a murine arthritis model, Front. Immunol. 10 (2019) 1–12.
[10] Z. Hunter, D.P. McCarthy, W.T. Yap, C.T. Harp, D.R. Getts, L.D. Shea, S.D. Miller, A biodegradable nanoparticle platform for the induction of antigen-specific immune tolerance for treatment of autoimmune disease, ACS Nano 8 (2014).
[11] N.A. Nagy, A.M. de Haas, T.B.H. Geijtenbeek, R. van Ree, S.W. Tas, Y. van Kooyk, E.C. de Jong, Therapeutic liposomal vaccines for dendritic cell activation or tolerance, Front. Immunol. 12 (2021) 1–16.
[12] A. Sonigra, H.J. Nel, P. Wehr, N. Ramnoruth, S. Patel, K.A. van Schie, M.W. Bladen, A.M. Mehdi, J. Tesiram, M. Talekar, J. Rossjohn, H.H. Reid, F.E. Stuurman, H. Roberts, P. Vecchio, I. Gourley, M. Rigby, S. Becart, R.E.M. Toes, H.U. Scherer, K.A.L. Cao, K. Campbell, R. Thomas, Randomized phase I trial of antigen-specific tolerizing immunotherapy with peptide/calcitriol liposomes in ACPA+ rheumatoid arthritis, JCI Insight 7 (2022).
[13] I. Garcia-Loza, D. Perna-Barrull, E. Aguilera, L. Almenara-Fuentes, L. Gomez-Muñoz, D. Greco, M. Vila, M. Salvado, M. Mancera-Arteu, M.W. Olszowy, J. Petriz, M. Dalmases, S. Rodriguez-Vidal, B. Barneda-Zahonero, M. Vives-Pi, Targeting macrophages with phosphatidylserine-rich liposomes as a potential antigen-specific immunotherapy for type 1 diabetes, J. Autoimmun. 145 (2024) 103196.
[14] N. Benne, J.J.H. Janssen, E. Mastrobattista, F. Broere, Direct immunomodulatory effects of DSPC:DSPG:CHOL liposomes on murine dendritic cells, Eur. J. Pharm. Sci. 212 (2025) 107201.

[15] N. Benne, D. ter Braake, D. Porenta, C.Y.J. Lau, E. Mastrobattista, F. Broere, Autoantigen-dexamethasone conjugate-loaded liposomes halt arthritis development in mice, Adv. Healthc. Mater. 13 (2024).
[16] C. Krienke, L. Kolb, E. Diken, M. Streuber, S. Kirchhoff, T. Bukur, Ö. Akilli-Öztürk, L.M. Kranz, H. Berger, J. Petschenka, M. Diken, S. Kreiter, N. Yogev, A. Waisman, K. Karikó, Ö. Türeci, U. Sahin, A noninflammatory mRNA vaccine for treatment of experimental autoimmune encephalomyelitis, Science 371 (2021) 145–153.
[17] A.-S. Bergot, I. Buckle, S. Cikaluru, J.L. Naranjo, C.M. Wright, G. Zheng, M. Talekar, E.E. Hamilton-Williams, R. Thomas, Regulatory T cells induced by single-peptide liposome immunotherapy suppress islet-specific T cell responses to multiple antigens and protect from autoimmune diabetes, J. Immunol. 204 (2020).
[18] L. Almenara-Fuentes, S. Rodriguez-Fernandez, E. Rosell-Mases, K. Kachler, A. You, M. Salvado, D. Andreev, U. Steffen, H. Bang, A. Bozec, G. Schett, R. Le Panse, J. Verdaguer, M. Dalmases, S. Rodriguez-Vidal, B. Barneda-Zahonero, M. Vives-Pi, A new platform for autoimmune diseases. Inducing tolerance with liposomes encapsulating autoantigens, Nanomedicine (London) 48 (2023), 102635–102635.
[19] D. Porenta, E. Lozano-Andrés, E. Mastrobattista, F. Broere, N. Benne, Detailed splenic single-cell biodistribution of phosphatidylglycerol-containing liposomes, Mol. Pharm. 23 (2026).
[20] R. Van Eenige, P.S. Verhave, P.J. Koemans, I.A.C.W. Tiebosch, P.C.N. Rensen, S. Kooijman, RandoMice, a novel, user-friendly randomization tool in animal research, PLoS One 15 (2020).
[21] S.E. Berlo, T. Guichelaar, C.B. Ten Brink, P.J. Van Kooten, F. Hauet-Broeren, K. Ludanyi, W. Van Eden, C.P. Broeren, T.T. Glant, Increased arthritis susceptibility in cartilage proteoglycan-specific T cell receptor-transgenic mice, Arthritis Rheum. 54 (2006) 2423–2433.
[22] A. Bendele, J. McComb, T. Gould, T. McAbee, G. Sennello, E. Chlipala, M. Guy, Animal models of arthritis: relevance to human disease, Toxicol. Pathol. 27 (1999) 134–142.
[23] J.D. Peterson, T.P. LaBranche, K.O. Vasquez, S. Kossodo, M. Melton, R. Rader, J. T. Listello, M.A. Abrams, T.P. Misko, Optical tomographic imaging discriminates between disease-modifying anti-rheumatic drug (DMARD) and non-DMARD efficacy in collagen antibody-induced arthritis, Arthritis Res. Ther. 12 (2010) R105.
[24] T.T. Glant, K. Mikecz, Proteoglycan aggrecan-induced arthritis: a murine autoimmune model of rheumatoid arthritis, Methods Mol. Med. 102 (2004) 313–338.
[25] C.S. Constantinescu, N. Farooqi, K. O'Brien, B. Gran, Experimental autoimmune encephalomyelitis (EAE) as a model for multiple sclerosis (MS), Br. J. Pharmacol. 164 (2011) 1079–1106.
[26] K. Almutairi, J. Nossent, D. Preen, H. Keen, C. Inderjeeth, The global prevalence of rheumatoid arthritis: a meta-analysis based on a systematic review, Rheumatol. Int. 41 (2021) 863–877.
[27] F.W. Miller, The increasing prevalence of autoimmunity and autoimmune diseases: an urgent call to action for improved understanding, diagnosis, treatment, and prevention, in: Current Opinion in Immunology, 2023.
[28] J.S. Smolen, Poor prognostic factors and unmet needs in rheumatoid arthritis, Rheumatology 64 (2025) ii3–ii8.
[29] J.S. Smolen, D. Aletaha, A. Barton, G.R. Burmester, P. Emery, G.S. Firestein, A. Kavanaugh, I.B. McInnes, D.H. Solomon, V. Strand, K. Yamamoto, Rheumatoid arthritis, Nat. Rev. Dis. Primers 4 (2018) 18001.
[30] T. Daemen, M. Velinova, J. Regts, M. De Jager, R. Kalicharan, J. Donga, J.J.L. Van Der Want, G.L. Scherphof, Different intrahepatic distribution of phosphatidylglycerol and phosphatidylserine liposomes in the rat, Hepatology 26 (1997).
[31] C. Oussoren, J. Zuidema, D.J.A. Crommelin, G. Storm, Lymphatic uptake and biodistribution of liposomes after subcutaneous injection. II. Influence of liposomal size, lipid composition and lipid dose, Biochim. Biophys. Acta Biomembr. 1328 (1997).
[32] J.M. Brewer, K.G.J. Pollock, L. Tetley, D.G. Russell, Vesicle size influences the trafficking, processing, and presentation of antigens in lipid vesicles, J. Immunol. 173 (2004) 6143–6150.
[33] S.H. Kim, J.H. Moon, S.U. Jeong, H.H. Jung, C.S. Park, B.Y. Hwang, C.K. Lee, Induction of antigen-specific immune tolerance using biodegradable nanoparticles containing antigen and dexamethasone, Int. J. Nanomedicine 14 (2019) 5229–5242.
[34] K. Doffek, X. Chen, S.L. Sugg, J. Shilyansky, Phosphatidylserine inhibits NFκB and p38 MAPK activation in human monocyte derived dendritic cells, Mol. Immunol. 48 (2011).
[35] N. Benne, J. van Duijn, F. Lozano Vigario, R.J.T. Leboux, P. van Veelen, J. Kuiper, W. Jiskoot, B. Slütter, Anionic 1,2-distearoyl-sn-glycero-3-phosphoglycerol (DSPG) liposomes induce antigen-specific regulatory T cells and prevent atherosclerosis in mice, J. Control. Release 291 (2018) 135–146.
[36] N.A. Nagy, C. Castenmiller, F.L. Vigario, R. Sparrius, T.M.M. van Capel, A.M. de Haas, Y. van Kooyk, R. van Ree, S.W. Tas, T.B.H. Geijtenbeek, W. Jiskoot, B. Slütter, E.C. de Jong, Uptake kinetics of liposomal formulations of differing charge influences development of in vivo dendritic cell immunotherapy, J. Pharm. Sci. 111 (2022) 1081–1091.
[37] R. Pattipeiluhu, G. Arias-Alpizar, G. Basha, K.Y.T. Chan, J. Bussmann, T.H. Sharp, M.-A. Moradi, N. Sommerdijk, E.N. Harris, P.R. Cullis, A. Kros, D. Witzigmann, F. Campbell, Anionic lipid nanoparticles preferentially deliver mRNA to the hepatic reticuloendothelial system, Adv. Mater. (Deerfield Beach, Fla.) 34 (2022) e2201095–e2201095.
[38] R. Tada, K. Nagao, R. Tanaka, S. Yamada, A. Watanabe, Y. Negishi, Involvement of splenic marginal zone macrophages in the recognition of systemically administered phosphatidylserine-coated liposomes in mice, Int. Immunopharmacol. 112 (2022) 109209.
[39] J.R. Melamed, J. Muscat-Rivera, M. Kegel, L.S. Chaboub, R. Perez-Tremble, N. S. Bhalla, H. Ni, H. Sun, D. Weissman, Anionic Lipids Modulate mRNA-Lipid Nanoparticle Immunogenicity and Confer Protection in a Mouse Model of Multiple Sclerosis, 2025.
[40] R. Cabezo'n, E.A. Carrera-Silva, G. Flo'rez-Grau, A.E. Errasti, E. Caldero'n-Go'mez, J.J. Lozano, C. Espan~a, E. Ricart, J.n. Pane's, C.V. Rothlin, D. Beni'tez-Ribas, MERTK as negative regulator of human T cell activation, J. Leukoc. Biol. 97 (2015).
[41] P.A. García-González, K. Schinnerling, A. Sepúlveda-Gutiérrez, J. Maggi, A. M. Mehdi, H.J. Nel, B. Pesce, M.L. Larrondo, O. Aravena, M.C. Molina, D. Catalán, R. Thomas, R.A. Verdugo, J.C. Aguillón, Dexamethasone and monophosphoryl lipid a induce a distinctive profile on monocyte-derived dendritic cells through transcriptional modulation of genes associated with essential processes of the immune response, Front. Immunol. 8 (2017).
[42] G. De Couto, E. Jaghatspanyan, M. Deberge, W. Liu, K. Luther, Y. Wang, J. Tang, E. B. Thorp, E. Marbán, Mechanism of enhanced MerTK-dependent macrophage efferocytosis by extracellular vesicles, Arterioscler. Thromb. Vasc. Biol. 39 (2019).
[43] L. Zhang, M. DeBerge, J. Wang, A. Dangi, X. Zhang, S. Schroth, Z. Zhang, E. B. Thorp, X. Luo, Receptor tyrosine kinase MerTK suppresses an allogenic type I IFN response to promote transplant tolerance, Am. J. Transplant. 19 (2019).
[44] V. Li, M.D. Binder, T.J. Kilpatrick, The tolerogenic influence of dexamethasone on dendritic cells is accompanied by the induction of efferocytosis, promoted by MERTK, Int. J. Mol. Sci. 24 (2023).
[45] M.D. Binder, E.C. Nwoke, E. Morwitch, C. Dwyer, V. Li, A. Xavier, R.A. Lea, J. Lechner-Scott, B.V. Taylor, A.L. Ponsonby, T.J. Kilpatrick, HLA-DRB1*15:01 and the MERTK gene interact to selectively influence the profile of MERTK-expressing monocytes in both health and MS, Neurology(R) Neuroimmunol. Neuroinflam. 11 (2024).
[46] D. Rozkova, R. Horvath, J. Bartunkova, R. Spisek, Glucocorticoids severely impair differentiation and antigen presenting function of dendritic cells despite upregulation of Toll-like receptors, Clin. Immunol. 120 (2006) 260–271.
[47] I. Rivero Berti, R.C. Gambaro, M.J. Limeres, C. Huck-Iriart, M. Svensson, S. Fraude-El Ghazi, L. Pretsch, S. Si, I. Lieberwirth, K. Landfester, M.L. Cacicedo, G.A. Islan, S. Gehring, Encapsulation of dexamethasone into mRNA-lipid nanoparticles is a promising approach for the development of liver-targeted anti-inflammatory therapies, Int. J. Mol. Sci. 25 (2024).
[48] F. Mannara, T. Valente, J. Saura, F. Graus, A. Saiz, B. Moreno, Passive experimental autoimmune encephalomyelitis in C57BL/6 with MOG: evidence of involvement of B cells, PLoS One 7 (2012) e52361.
[49] J. Pfeil, M. Simonetti, U. Lauer, B. von Thülen, P. Durek, C. Poulsen, J. Pawlowska, M. Kröger, R. Krähmer, F. Leenders, U. Hoffmann, A. Hamann, Prevention of EAE by tolerogenic vaccination with PEGylated antigenic peptides, Ther. Adv. Chronic Dis 12 (2021), 20406223211037830.
[50] G. Cappellano, A.D. Woldetsadik, E. Orilieri, Y. Shivakumar, M. Rizzi, F. Carniato, C.L. Gigliotti, E. Boggio, N. Clemente, C. Comi, C. Dianzani, R. Boldorini, A. Chiocchetti, F. Renò, U. Dianzani, Subcutaneous inverse vaccination with PLGA particles loaded with a MOG peptide and IL-10 decreases the severity of experimental autoimmune encephalomyelitis, Vaccine 32 (2014) 5681–5689.
[51] X. Xu, X. Wang, Y.-P. Liao, L. Luo, T. Xia, A.E. Nel, Use of a liver-targeting immune-tolerogenic mRNA lipid nanoparticle platform to treat peanut-induced anaphylaxis by single- and multiple-epitope nucleotide sequence delivery, ACS Nano 17 (2023) 4942–4957.
[52] T.L. Nguyen, Y. Choi, J. Im, H. Shin, N.M. Phan, M.K. Kim, S.W. Choi, J. Kim, Immunosuppressive biomaterial-based therapeutic vaccine to treat multiple sclerosis via re-establishing immune tolerance, Nat. Commun. 13 (2022).
[53] C.P. Kelly, J.A. Murray, D.A. Leffler, D.R. Getts, A.C. Bledsoe, G. Smithson, M. R. First, A. Morris, M. Boyne, A. Elhofy, T.T. Wu, J.R. Podojil, S.D. Miller, TAK-101 nanoparticles induce gluten-specific tolerance in celiac disease: a randomized, double-blind, placebo-controlled study, Gastroenterology 161 (2021) 66–80.e68.
[54] H.O. Alsaab, F.D. Alharbi, A.S. Alhibs, N.B. Alanazi, B.Y. Alshehri, M.A. Saleh, F. S. Alshehri, M.A. Algarni, T. Almugaiteeb, M.N. Uddin, R.M. Alzhrani, PLGA-based nanomedicine: history of advancement and development in clinical applications of multiple diseases, Pharmaceutics 14 (2022) 2728.
[55] M. Chen, D. Jia, Y. Wu, K. Wang, X. Zhao, X. Guo, S. Zhou, Tolerogenic nanovaccine synergizing citrullinated peptide and TSP-1 plasmid for antigen-specific immunotherapy of rheumatoid arthritis, Small 0 (2026) e73817.
[56] E.M. Delemarre, T. van den Broek, G. Mijnheer, J. Meerding, E.J. Wehrens, S. Olek, M. Boes, M.J.C. van Herwijnen, F. Broere, A. van Royen, N.M. Wulffraat, B. J. Prakken, E. Spierings, F. van Wijk, Autologous stem cell transplantation aids autoimmune patients by functional renewal and TCR diversification of regulatory T cells, Blood 127 (2016) 91–101.
[57] J. Tian, J. Yong, H. Dang, D.L. Kaufman, Oral GABA treatment downregulates inflammatory responses in a mouse model of rheumatoid arthritis, Autoimmunity 44 (2011) 465–470.
[58] K. Mikecz, T.T. Glant, A. Markovics, K.S. Rosenthal, J. Kurko, R.E. Carambula, S. Cress, H.L. Steiner, D.H. Zimmerman, An epitope-specific DerG-PG70 LEAPS vaccine modulates T cell responses and suppresses arthritis progression in two related murine models of rheumatoid arthritis, Vaccine 35 (2017) 4048–4056.
[59] D.H. Zimmerman, K. Mikecz, A. Markovics, R.E. Carambula, J.C. Ciemielewski, D. M. Toth, T.T. Glant, K.S. Rosenthal, Vaccination by two DerG LEAPS conjugates incorporating distinct proteoglycan (PG, aggrecan) epitopes provides therapy by different immune mechanisms in a mouse model of rheumatoid arthritis, Vaccines 9 (2021) 448.

[60] E. Neumann, S. Lefèvre, B. Zimmermann, S. Gay, U. Müller-Ladner, Rheumatoid arthritis progression mediated by activated synovial fibroblasts, Trends Mol. Med. 16 (2010) 458–468.
[61] T.K. Rasmussen, T. Andersen, M. Hvid, M.L. Hetland, K. Hørslev-Petersen, K. Stengaard-Pedersen, C.K. Holm, B. Deleuran, Increased interleukin 21 (IL-21) and IL-23 are associated with increased disease activity and with radiographic status in patients with early rheumatoid arthritis, J. Rheumatol. 37 (2010) 2014–2020.
[62] Q. Niu, B. Cai, Z.C. Huang, L.I. Wang, Y.Y. Shi, Disturbed Th17/Treg balance in patients with rheumatoid arthritis, Rheumatol. Int. 32 (2012) 2731–2736.
[63] K. Raza, C.E. Buckley, M. Salmon, C.D. Buckley, Treating very early rheumatoid arthritis, Best Pract. Res. Clin. Rheumatol. 20 (2006) 849–863.
[64] L. Bevaart, M.J. Vervoordeldonk, P.P. Tak, Evaluation of therapeutic targets in animal models of arthritis: how does it relate to rheumatoid arthritis? Arthritis Rheum. 62 (2010) 2192–2205.
[65] A. Tracy, C.D. Buckley, K. Raza, Pre-symptomatic autoimmunity in rheumatoid arthritis: when does the disease start? Semin. Immunopathol. 39 (2017) 423–435.